Window Function for EEG Power Density Estimation and Its Application in SSVEP Based BCIs

Conference Paper · December 2011

DOI: 10.1007/978-3-642-25489-5_14 · Source: DBLP

CITATIONS
4

READS
479

4 authors:

Gan Huang

38 PUBLICATIONS **582** CITATIONS

SEE PROFILE

Meng Jianjun

Shanghai Jiao Tong University

39 PUBLICATIONS **696** CITATIONS

SEE PROFILE

Dingguo Zhang

University of Bath

192 PUBLICATIONS **2,061** CITATIONS

SEE PROFILE

Xiangyang Zhu

Shanghai Jiao Tong University

210 PUBLICATIONS **2,667** CITATIONS

SEE PROFILE

Window Function for EEG Power Density Estimation and Its Application in SSVEP Based BCIs

Gan Huang, Jianjun Meng, Dingguo Zhang, and Xiangyang Zhu

State Key Laboratory of Mechanical System and Vibration
Shanghai Jiao Tong University
Shanghai, China, 200240
huanggan1982@gmail.com
http://www.robot.sjtu.edu.cn

Abstract. A high quality power density estimation for certain frequency components in a short time is of key importance in Steady-State Visual Evoked Potentials (SSVEP) based Brain Computer Interface (BCI). In this paper, the effect of the window functions in SSVEP based BCIs is discussed. EEG signal is a typical color noise with a high energy of the low frequency component. The main findings are that (1) The spectral leakage for EEG signals has some regular patterns. An obvious oscillation with the corresponding frequency can be observed. The amplitude of the oscillation decreases with the growth of the frequency. A short analysis is also given for the leakage. (2) The leakage from the low frequency component can be effectively suppressed by the using of some windows, such as Hamming, Hann and triangle window; (3) By removing the influence of the leakage from the low frequency component with high pass filter, the classification results are mainly determined by the width of the main lobe. The rectangle window would have a better accuracy than Hamming, Hann and triangle window. Some windows constructed with a narrower main lobe width have a potential use in SSVEP based BCIs.

Keywords: SSVEP, EEG, Lowpass Filter, STFT.

1 Introduction

Brain Computer Interface (BCI), which has been developed fast in recent years, provides human beings direct ways to communicate with computer by intent alone. This new communication way is hoped to help the patients with sever neuromuscular disorders, such as late-stage amyotrophic lateral sclerosis, severe cerebral palsy, head trauma, and spinal injuries in the daily life. Several electrophysiological sources can be used for BCI control, including Event-Related Synchronization/Desynchronization (ERS/ERD), Steady-State Visual Evoked Potentials (SSVEP), Slow Cortical Potentials (SCP), P300 evoked potentials and μ and β rhythms [1]. Encouraged by the advantage of less training time [2–4], shorter response time [5] and higher information transfer rates [2, 6], SSVEP

S. Jeschke, H. Liu, and D. Schilberg (Eds.): ICIRA 2011, Part II, LNAI 7102, pp. 135–144, 2011.

based BCIs are more suitable to be developed in real time controlling. In recent years, SSVEP based BCIs used in cursor control [7], prosthetic control [8] and Functional Electrical Stimulation (FES) [9] have been reported. Some combination BCIs, based on SSVEP and other sources, have also been developed [10].

SSVEP is a continuous steady brain response for a repetitive stimulus with a certain frequency. It is mainly observed in visual and parietal cortical area. Occasionally, a smaller response is also observed in the mid-frontal region [11]. In SSVEP based BCIs, visual stimulus with different frequencies are simultaneously presented to the user. Each visual stimulus is associated with a command in an output (active) device. The user selected command can be detected as a larger maximum of the same frequency (and its harmonics) is found in the brain activity. Hence, the high quality power density estimation for certain frequency components in a short time is of key importance in SSVEP based BCIs.

In most SSVEP based BCIs, Fourier-related transforms are used widely in power density estimation[3, 5, 6, 8]. To estimate the power density at certain frequency ω of the signal in the vicinity of time t, Short-Time Fourier Transform (STFT) is used in this work. STFT is a Fourier-related transform used to determine the amplitude and phase-frequency distributions of local sections of a signal as it changes over time. In the continuous-time case, the STFT of signal $x(t)$ is written as

$$\mathrm{STFT}_x(t,\omega) = \int_{-\infty}^{\infty} x(\tau)w(\tau,t)e^{-j2\pi\omega\tau}d\tau,$$

where $w(s,t)$ is the window function which is nonzero for only a short period of time $s \in [t - L/2, t + L/2]$, L is the size of the window. The power density estimation of frequency ω at time t is

$$P_\omega(t) = \frac{1}{L}\left|\mathrm{STFT}_x(t,\omega)\right|^2 = \frac{1}{L}\left|\int_{-\infty}^{\infty} x(\tau)w(\tau,t)e^{-j2\pi\omega\tau}d\tau\right|^2.$$

Because of the signal truncation in STFT, the spectral leakage problem will occur. It appears as if some energy has "leaked" out from the true frequency of the signal into adjacent frequencies. To help reduce the spectral leakage, the window functions are used. The rectangular window with a narrow main lobe has excellent resolution characteristics for comparable strength signals with similar frequencies, but it is a poor choice for noise suppression. Flat top window have low side lobe peak, which does not provide well a frequency resolution but can measure the strength of a signal accurately at any frequency. Between the extremes, some moderate windows, such as Hamming, Hann and triangle windows, are used commonly as a tradeoff among narrow main lobe (corresponding to high frequency resolution), low side lobe peak and rapidly fall-off side lobes (corresponding to noise suppression). In the application of SSVEP based BCI, to get the transient response of the subjects and also as the simplest window, rectangular window have been widely used [3, 5, 6, 8, 9, 12]. Some other windows, like Hamming [7] and Gaussian windows [13], are also used in their applications.

In this paper, we study the effect of window function on power density estimation of EEG signals. In the following, the experiment is introduced in Section 2. The characteristic of EEG signals is introduced in Section 3. The spectral leakage problem and the use of window function are also discussed. In Section 4, we apply these methods in the SSVEP based BCI system to test the use of window function. Section 5 is the conclusion.

2 Experiment Setting

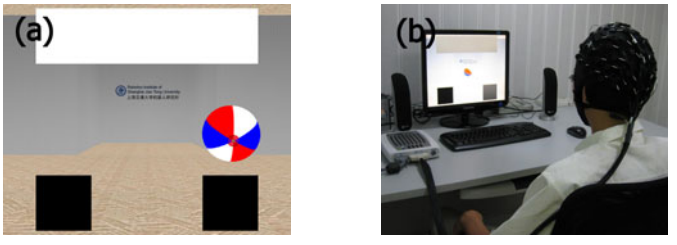

Fig. 1. (a) A screenshot during the experiment. The rectangles in the left, up and right of the screen flick with the frequencies 5, 8.33 and 12.5Hz. During the experiment, the subjects would watch the corresponding flicking bar as the color ball indicated. (b) The experimental environment. The subjects were seated in a comfortable armchair in an electrically shielded room with the light on. 6 channel signals from occipital area were recorded for analysis.

2.1 Subjects

Six subjects, aged from 22-28 years, participated in the experiment. All participants were seated in a comfortable armchair in an electrically shielded room and viewed a 19 inches LCD display at a distance of 1m (Fig. 1(b)). The light is always on during the experiment. The subjects were instructed to keep still and try to avoid blinking during the experiment, but a habitually blinking was still observed from subject LJW and SXZ.

2.2 EEG Recording

EEG signals were recorded using a SynAmps system (Neuroscan, USA). Signals from channel P3, Pz, P4, O1, Oz and O2 were recorded for analysis (Fs=1000samples/s, 0.05-200Hz). The grounding electrode was mounted on the forehead and reference electrodes between position Cz and CPz according to the system of electrode placement described in [14]. The electrodes were placed according to the extended 10/20-system.

2.3 Experimental Paradigms

As shown in Fig. 1(a), the experiment was set up in a virtual room, and three flicking bars with their frequencies 5, 8.33 and 12.5Hz was placed in the left, up and right of the screen. The monitor was with the refresh rate 75Hz. The experiment consisted of 3 sections with 90 seconds per section. In each section, a color ball appeared in the left, right or front of the screen, which would be changed randomly every 5 seconds. The subjects were asked to watch the corresponding flicking bar.

3 EEG Signal and Window Function

The signal displayed in Fig.2 is a typical EEG signal at channel Oz with 6 seconds length without visual stimulus. The spectral characteristics are shown in the subfigure. The energy of the low frequency components is much higher than others. It can be treated as a color noise.

Fig. 3(a) shows the power density function $P_\omega(t)$ of the signal in Fig.2 at certain frequencies (ω =8Hz, 10Hz, 12Hz, 14Hz and 16Hz), in which the rectangle window is used with the window size $L = 1s$ for $t \in [0.5, 5.5]$. Due to the high energy of the low frequency components, the spectral leakage problem in the power density estimation is serious. Unlike the power density estimation of white noise, the leakage in the EEG like color noise has some regular patterns. As shown Fig. 3(a), an obvious oscillation is observed in the power density estimation of all the frequency compontents. The oscillation of $P_\omega(t)$ at frequency $\omega = 16$Hz is faster but smaller than it at frequency $\omega = 10$Hz and $\omega = 8$Hz. Taking FFT on $P_\omega(t)$, Fig.3(b) shows the Power Spectrum Density (PSD) of $P_\omega(t)$, denoted by $\mathrm{PSD}_{P_\omega}(\Omega)$. It is clear that the oscillation frequency of $P_\omega(t)$ is related to its frequency ω. The amplitude of the oscillation decreases with the growth of ω. Lower frequencies will make a larger oscillation.

The following analysis will make us understand the oscillation. Let the signal $x(t) = \sin(2\pi\omega_0 t)$ to be used to present the low frequency component with ω_0 close to 0. The rectangle windows is represented as

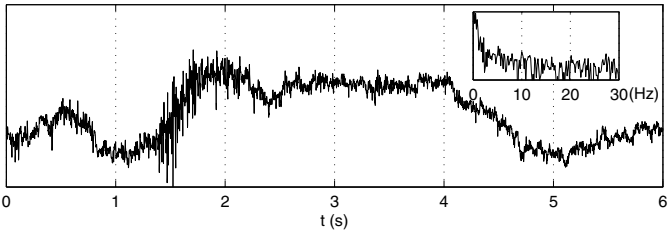

Fig. 2. Typical EEG signals with 6 seconds length without visual stimulus. The subfigure is the frequency spectrum for 0 to 30 Hz. It can be seened as a color noise with the high energy of low frequency components.

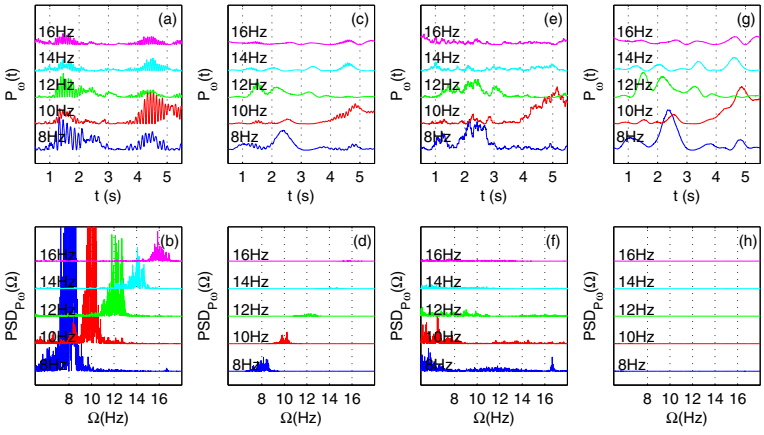

Fig. 3. A comparison of the effect of the window function and high pass filter in the power spectral density estimation of the real EEG signals. The figures in the left show the time-frequency property $P_\omega(t)$ of the signal, and the right figures are the corresponding power spectrum density of $P_\omega(t)$, $\mathrm{PSD}_{P_\omega}(\Omega)$. In fig. (a) and (b), the rectangular window is used without high pass filter. In fig. (c) and (d), the hamming window is used with no high pass filter. In fig. (e) and (f), the rectangular window is used with the 4-order butterworth high pass filter with the cutoff frequency 2Hz. In fig. (g) and (h), the hamming window is used with the 4-order butterworth high pass filter with the cutoff frequency 2Hz. The window size $L = 1.0s$.

$$w(s,t) = \begin{cases} 1 & s \in [t - L/2, t + L/2], \\ 0 & else. \end{cases}$$

The Fourier transformation for $x(t)$ and $w(s,t)$ is

$$\mathcal{F}_x(t,\omega) = X(\omega) = \tfrac{1}{2}j[\delta(\omega+\omega_0) - \delta(\omega-\omega_0)],$$
$$\mathcal{F}_w(t,\omega) = W(t,\omega) = \tfrac{1}{2j\pi\omega}e^{-j2\pi\omega t}[e^{j\pi\omega l} - e^{-j\pi\omega l}] = \tfrac{1}{\pi\omega}e^{-j2\pi\omega t}\sin(\pi\omega l),$$

where $\mathcal{F}_x(t,\omega)$ keeps unchanged with time t, and the amplitude of $\mathcal{F}_x(t,\omega)$ is a periodic function of t with the frequency ω. The STFT of the signal $x(t)$ can be expressed as

$$\begin{aligned} &\mathrm{STFT}_x(t,\omega) \\ &= \mathcal{F}_{x\cdot w}(t,\omega) \\ &= X(t,\omega) * W(t,\omega) \\ &= \textstyle\int_{-\infty}^{+\infty} X(\tau)W(t,\omega-\tau)d\tau \\ &= \tfrac{1}{2}j\textstyle\int_{-\infty}^{+\infty}[\delta(\tau+\omega_0) - \delta(\tau-\omega_0)]W(t,\omega-\tau)d\tau \\ &= \tfrac{1}{2}j[W(t,\omega+\omega_0) - W(t,\omega-\omega_0)] \end{aligned}$$

Considering the expression of $W(t,\omega+\omega_0)$ and $W(t,\omega-\omega_0)$, the leakage from the low frequency component $x(t)$ at frequency ω behaves as an oscillation at the

frequencies $\omega + \omega_0$ and $\omega - \omega_0$. If ω_0 is close to 0, the oscillation frequencies will be close to the frequency ω. The oscillation amplitude is larger as ω near $\pm\omega_0$, and decreases with ω getting away from $\pm\omega_0$. If the energy of frequency ω_0 is much larger than the other frequencies' energy, the oscillation will be observed. This coincides with the power density estimation result in Fig. 3(a).

In STFT, all the data points outside the window are truncated and therefore assumed to be zero, which leads to the spectral leakage problem in the power density estimation. The leakage is unavoidable with the use of window function. But some window functions with low level of the side lobes can reduce the leakage. As shown in Fig. 3(c) and (d), the use of hamming window can make the oscillation weaken but never fade away.

Due to the oscillation caused by the high energy of the low frequency component, high pass filters provide a directly way to solve this problem. In Fig. 3(e) and (f), a 4-order butterworth high pass filter with the cutoff frequency 2Hz is applied before the power density estimation. The curves $P_\omega(t)$ in Fig. 3(e) are not smoother than those in Fig. 3(c). But the oscillation related to the frequency ω is suppressed effectively, while the oscillation in other frequencies still exists.

The combination of high pass filter and hamming window can make the estimation curves even more smooth in Fig. 3(g). Its power spectral density $\mathrm{PSD}_{P_\omega}(\Omega)$ in Fig. 3(h) shows that the oscillation with both frequency ω and the other frequencies are effectively suppressed.

4 Application in SSVEP

Table 1. The classification accuracies with different window functions before and after high pass filter in six subjects. Four type of window functions are compared, which is rectangle, Hamming, Hann and triangle window. The high pass filter here is the 4-order butterworth high pass filter with the cutoff frequency 2Hz. The maximum value of the accuracy among the four windows is marked in bold.

subject	no filter				high pass filter			
	rectangle	hamming	hann	triangle	rectangle	hamming	hann	triangle
HPH	71.78	**80.00**	**80.00**	**80.00**	**80.37**	79.70	80.00	79.70
HG	86.59	88.74	88.37	**89.11**	**92.44**	88.89	88.22	89.11
LJW	77.19	88.52	87.70	**89.56**	**90.89**	88.81	87.70	89.41
PLZ	**99.56**	99.19	99.19	99.19	**99.33**	99.19	99.19	99.19
SXZ	48.15	**69.48**	69.26	69.33	**77.04**	71.93	69.33	71.56
YL	91.93	92.89	91.93	**93.19**	**93.85**	92.74	91.93	93.11
mean	78.98	86.47	86.07	**86.73**	**88.99**	86.88	86.06	87.01

4.1 Method

In this section, the effects of several window functions the power spectral density estimation are compared before and after and high pass filters in the application of SSVEP. As mentioned in Section 2.3, subjects are asked to focus on the targeted flicking bars, which will change every 5 seconds. From $t \in [1.5, 4]$, the power spectral density has been estimated in steps of 0.1 second (25 samples per 5 seconds). Hence there are 1350 samples in three classes for each subject. For each sample, the value of $|\mathrm{STFT}_x(t, \omega)|$ is calculated with 6 electrodes (P3, Pz, P4, O1, Oz and O2) at the characteristic frequencies and their harmonics (ω = 5, 8.33, 12.5 and 10, 16.67, 25Hz). Linear Discriminant Analysis (LDA) is used for classification [15, 16]. The accuracy rates are given by 3 fold cross validation (two sections are used to train, the remained section is retained as the validation data for testing).

4.2 Result

In Tab.1, the accuracy rates are compared with the four window functions (rectangle, Hamming, Hann and triangle windows) before and after the high pass filter. The window size $L = 1.0s$. The best classification result among the four windows is marked in bold. The high pass filter used is the 4-order butterworth high pass filter with the cutoff frequency 2Hz. Without high pass filter, the results with Hamming, Hann and triangle window are similar and better than those with rectangle window. After high pass filter, a 10% improvement is achieved for rectangle window in average. An extreme growth happens on subject SXZ, in which the high pass filter makes an approximate 30% increasement with rectangle window. In contrast, the results for other windows hold on or increase a little. Hence, the best accuracies for all subjects come from rectangle window. Some windows provide smoother power density estimations, such as hamming window shown in Fig. 3(g), fail to get a better accuracy after high pass filter, which does not meet our expectations.

In the following, we extend our test on more window functions and different window sizes. 17 window functions with their main lobe width and side lobe peaks are listed in Tab. 2 in descending order of the main lobe width. The first 16 window function are natively implemented in matlab. The last window "anti-flattopwin" is constructed by $1 - 0.7 \times \mathrm{window}(@\mathrm{flattopwin}, \mathrm{N})$, which has narrower main lobe but higher side lobe than rectangle window. N is the number of sampling points, which is related with the window size L and sampling rate Fs. Fig. 4 shows the average accuracies of six subjects with different main lobe width of the 17 windows for different window sizes (L=0.5, 1.0, 1.5 and 2.0s). The accuracies before and after high pass filter are correspondingly marked by blue star and red circle. The recognition rates increase for all windows with the growth of window size. For the windows with the -3dB main lobe width($\times 2\pi/N$) greater than 1, the accuracies before and after high pass filter are similar and decrease as the growth of the main lobe width. It indicates that if the side lobe below certain level, the spectral leakage from low frequency component have

Table 2. The 17 window function used in Fig. 4 with their -3dB main lobe width and side lobe peak. The "anti-flattopwin" is constructed by us with narrower main lobe width than rectangle windows.

window	-3dB main lobe width ($\times 2\pi/N$)	side lobe peak (dB)
flattopwin	3.72	-96.00
blackmanharris	1.90	-98.97
nuttallwin	1.87	-98.86
chebwin	1.84	-100.00
parzenwin	1.82	-53.05
bohmanwin	1.70	-46.00
blackman	1.64	-96.31
hann	1.44	-31.47
barthannwin	1.40	-35.88
gausswin	1.37	-43.30
hamming	1.30	-44.20
bartlett	1.27	-26.52
triang	1.27	-26.52
tukeywin	1.15	-15.12
kaiser ($\beta = 2$)	0.99	-18.45
rectwin	0.88	-13.26
anti-flattopwin	0.81	-7.72

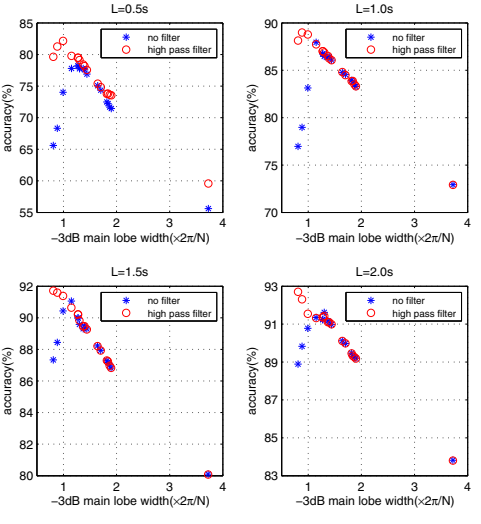

Fig. 4. The average classify results of the six subjects by using 17 window functions of different main lobe width. The results before and after high pass filters are marked by blue stars and red circles. The window size $L = 0.5, 1.0, 1.5, 2.0s$ in the subfigures from (a) to (d).

been suppressed effectively and a smaller side lobe would not help to improve the classication results any more. However the increasing of the main lobe width makes the windows' frequency domain resolution weaken, which leads to the decreasing of the accuracies. For the last three windows (kaiser, rectwin, anti-flattopwin) in Tab. 2, all of them have narrower main lobe width with larger side lobe. The spectral leakage from low frequency component is large enough for these windows to influence the classication results. The accuracies are improved greatly after high pass filter. The better accuracy is achieved by is a tradeoff with frequency domain resolution and spectral leakage. For shorter window size, such as $L = 0.5s$ in Fig. 4(a), a window with smaller side lobe is preferred. While a longer window size ($L = 1.5, 2.0s$ in Fig. 4(c) and (d)) could make the window with narrower main lobe improve their classication results. Some windows with narrower main lobes, like "anti-flattopwin", have their uses.

Remark1: In the comparison above, the "anti-flattopwin" has been constructed with a narrower main lobe than rectangle window. In fact, we can construct a series of windows in the following forms $1 - \alpha \times w(s,t)$ where $\alpha \in (0,1]$, w can be chosen from the first 15 windows listed in Tab. 2. As α grows from 0 to 1, these "anti" type windows have narrower main lobe but a higher side lobe. Take "anti-tukeywin" window with $\alpha = 1$ for example, -3dB main lobe width is $0.58(\times 2\pi/N)$, however the peak of the side lobe -0.62dB is real large, which is close to the main lobe.

Remark2: It's worth noting that although the side lobe peak of tukey window is larger than kaiser window, it is decayed much faster. Hence tukey window has less been influenced by high pass filter than kaiser window. The speed for the side lobes fall-off is not listed in Tab. 2, because for some windows, like "nuttallwin", "blackmanharris", "flattopwin" the peaks of the side lobes is not monotonically decreasing.

5 Conclusion

In this paper, we discussed the use of the window function in the application of SSVEP based BCIs. An ideal window function should have a narrow main lobe and low side lobes. In the noisy circumstances, the lower side lobes could reduce the impact of spectral leakage to the accuracy. And the narrower main lobe could provide a higher frequency domain solution, which leads to a better transient response. However, it is impossible for a window to satisfy both parties. The choice of the windows is to determine the quality of the signals. The windows with high frequency domain solution could be used to improve the classification results if the Signal to Noise Ratio (SNR) has been improved by some methods, such as high pass filter used here.

Acknowledgment. This work is supported by National High Technology Research and Development Program of China (No. 2009AA04Z212), National Natural Science Foundation of China (No.51075265), and Science Technology Commission of Shanghai Municipality (No.09JC1408400).

References

1. Wolpaw, J.R., Birbaumer, N., McFarland, D.J., Pfurtscheller, G., Vaughan, T.M.: Brain-computer interfaces for communication and control. Clinical Neurophysiology 113(6), 767–791 (2002)
2. Garcia, G.: High frequency SSVEPs for BCI applications, In: Computer-Human Interaction (2008)
3. Lin, Z., Zhang, C., Wu, W., Gao, X.: Frequency recognition based on canonical correlation analysis for SSVEP-based BCIs. IEEE Transactions on Biomedical Engineering 54(6), 1172–1176 (2007)
4. Wu, Z., Yao, D.: Frequency detection with stability coefficient for steady-state visual evoked potential (SSVEP)-based BCIs. Journal of Neural Engineering 5, 36 (2008)
5. Pfurtscheller, G., Solis-Escalante, T., Ortner, R., Linortner, P.: Self-Paced Operation of an SSVEP-Based Orthosis With and Without an Imagery-Based" Brain Switch": A Feasibility Study Towards a Hybrid BCI. IEEE Transactions on Neural Systems and Rehabilitation Engineering: a Publication of the IEEE Engineering in Medicine and Biology Society 18(4), 409–414 (2010)
6. Cheng, M., Gao, X., Gao, S., Xu, D.: Design and implementation of a brain-computer interface with high transfer rates. IEEE Transactions on Biomedical Engineering 49(10), 1181–1186 (2002)
7. Trejo, L.J., Rosipal, R., Matthews, B.: Brain–computer interfaces for 1-D and 2-D cursor control: designs using volitional control of the EEG spectrum or steady-state visual evoked potentials. IEEE Transactions on Neural Systems and Rehabilitation Engineering 14(2), 225 (2006)
8. Muller-Putz, G.R., Pfurtscheller, G.: Control of an electrical prosthesis with an SSVEP-based BCI. IEEE Transactions on Biomedical Engineering 55(1), 361–364 (2008)
9. Gollee, H., Volosyak, I., McLachlan, A., Hunt, K., Graser, A.: An SSVEP based brain-computer interface for the control of functional electrical stimulation. IEEE Transactions on Bio-Medical Engineering 57(8), 1847–1855 (2010)
10. Edlinger, G., Groenegress, C., Prückl, R., Guger, C., Slater, M.: Goal orientated Brain-Computer interfaces for Control: a virtual smart home application study. BMC Neuroscience 11(suppl. 1), 134 (2010)
11. Burkitt, G.R., Silberstein, R.B., Cadusch, P.J., Wood, A.W.: Steady-state visual evoked potentials and travelling waves. Clinical Neurophysiology 111(2), 246–258 (2000)
12. Friman, O., Volosyak, I., Graser, A.: Multiple channel detection of steady-state visual evoked potentials for brain-computer interfaces. IEEE Transactions on Biomedical Engineering 54(4), 742–750 (2007)
13. Cui, J., Wong, W.: The adaptive chirplet transform and visual evoked potentials. IEEE Transactions on Biomedical Engineering 53(7), 1378–1384 (2006)
14. Chatrian, G.E., Lettich, E., Nelson, Ten, P.L.: percent electrode system for topographic studies of spontaneous and evoked EEG activity. Am J. EEG Technol. 25, 83–92 (1985)
15. Krzanowski, W.J.: Principles of multivariate analysis: a user's perspective. Oxford University Press, USA (2000)
16. Seber, G.A.F.: Multivariate Observations (1984)